Investigation of the Characteristics of the Boron Doped MnO Films Deposited by Spray Pyrolysis Method

M. Bedir[a], A. Tunç[a] and M. Öztas[b,*]

[a]University of Gaziantep, Deparment of Physics Engineering, Gaziantep, Turkey

[b]University of Yalova, Chemical and Process Engineering, Yalova, Turkey

(Received April 28, 2015; in final form September 21, 2015)

Boron doped MnO films were prepared by spray pyrolysis technique at 375 °C substrate temperature, which is a low cost and large area technique to be well-suited for the manufacture of solar cells, using boric acid (H_3BO_3) as dopant source, and their properties were investigated as a function of doping concentration. Boron doping was achieved by adding 0.1 M, 0.2 M, 0.3 M, and 0.4 M H_3BO_3 to the starting solution. X-ray analysis showed that the films were polycrystalline fitting well with a cubic structure and have preferred orientation in (111), (220) and (311) directions. Optical band gap of the undoped and B-doped MnO films were found to vary from 2.25 to 2.54 eV. The changes observed in the energy band gap and structural properties of the films related to the boric acid concentration are discussed in detail.

DOI: 10.12693/APhysPolA.129.1159

PACS/topics: 71.20.Nr, 78.20.–e

1. Introduction

The polycrystalline semiconductors have attracted much interest in an expanding variety of applications in various electronic and optoelectronic devices. The technological interest in polycrystalline-based devices is mainly caused by their very low production costs. Considerable attention has been paid to doped semiconductors as they offer multifunctional properties beyond those of ideal semiconductors [1]. In general, the characteristics of the films and related applications have been dominated by several factors, such as grain boundary, grain size, crystallinity, resistivity and optical and magnetic permeability, which are interrelated with utilized deposition and treatment methods and their variables [2–4]. In particular, materials known as diluted magnetic semiconductors (DMSs) which have an interesting combination of magnetism and semiconductivity, have attracted widespread scientific attention due to their prospective applications in magneto-optical and spintronic devices. In DMSs, the band electrons and holes strongly interact with the localized magnetic moments and cause a variety of interesting phenomena [2, 3].

MnO and boron doped MnO films can be prepared by different techniques such as radiofrequency sputtering [5], solvothermal synthesis [6], hydrothermal method [7], molecular beam epitaxy [8], thermal vacuum evaporation [9], successive ionic layer adsorption and reaction (SILAR) [10], chemical bath deposition (CBD) [11], and spray pyrolysis [12, 13]. Manganese oxide (MnO) is a transitional material having interesting physical and chemical properties. It has optoelectronic applications and is often used in electrode materials [14, 15], electrochemical capacitors [16, 17], rechargeable batteries, sensors [18], magnetoelectronic devices [19].

According to our knowledge, no report exists in the literature on the synthesis of boron doped MnO films by spray pyrolysis technique. Therefore, we have turned our attention to the study of the feasibility of spray pyrolysis technique for the synthesis of MnO:B films. In this study, the sprayed MnO:B films were developed in science park and investigations of the influence of boric acid concentration on the structural and optical properties of sprayed MnO:B films are reported.

2. Experimental details

Spray pyrolysis is basically a chemical process, which consists of a solution that is sprayed into a substrate held at high temperature, where the solution reacts forming the desired thin film. In this technique, the MnO:B films were deposited on heated microscope glass (Objekttrager, 1 cm×1 cm) substrates by spraying an aqueous solution in air atmosphere. The spray solutions are comprised of manganese chloride (0.5 M, Merck, $\geq$ 99%) and boric acid (H_3BO_3) as dopant source in the deionized water. The substrate temperature 375 °C was used and the temperature was controlled within ±5 °C through a chromel-alumel thermocouple as a sensor for the temperature controller. Before deposition, the glass substrates were ultrasonically cleaned in acetone solution, and then rinsed in deionized water. The distance between nozzle and substrate was about 35 cm. The prepared solution is sprayed (5 ml/min) onto the clean glass substrates with a deposition time ranged between 0.5 and 2.5 h. Boron doping was achieved by adding different molarities (0.1, 0.2, 0.3, and 0.4 M, respectively) of H_3BO_3 into the starting solution, which included manganese chloride ($MnCl_2$) at 1 M concentration in 100 ml deionized water.

*corresponding author; e-mail: mustafa.oztas@yalova.edu.tr

In this procedure, compressed air was used to atomize the solution containing the precursor compounds through a spray nozzle over the heated substrate; air is compressed from the atmosphere. The precursor is pyrolyzed on the heated substrate. The solution was pumped into the air stream in the spray nozzle by means of a syringe pump. The formation of boron doped MnO resulted from the chemical reaction

$$MnCl_{2(s)} + H_3BO_{3(s)} + H_2 \rightarrow$$

$$O_{(l)}MnO : B_{(s)} + 2HCl_{(g)} + 3OH^-_{(aq)}.$$

The analyses of these films are investigated in science park. The structural characterization of deposited films was made by X-ray diffraction (XRD) technique on Bruker AXS D5005 diffractometer (monochromatic Cu K_α radiation, $\lambda = 1.54056$ Å). Perkin Elmer Lambda 25 UV-VIS-NIR was used to determine the optical absorbance of the films as a function of wavelength at room temperature. The optical band-gap energy E_g was determined by extrapolating the high absorption region of the curve to the photon energy axis [20].

3. Results and discussion

3.1. Structural studies

Figure 1 shows the X-ray diffraction patterns of B-doped MnO films with different boron concentrations deposited at substrate temperature 375 °C. The diffraction pattern exhibits peaks at $2\theta = 28.4098°$, $2\theta = 47.2858°$ and $2\theta = 56.0638°$ which were identified to be (111), (220) and (311) planes. This indicates that the MnO:B films prepared by spray pyrolysis method are polycrystalline with the cubic structure and show a good *c*-axis orientation perpendicular to the substrate. It indicates that most of the grains in MnO:B films have a strong orientation along (111) and (220) planes as shown in Fig. 1. While the intensity of (111) and (220) peaks increases with increase of boron concentration up to 0.1 M, then the intensity of (111) and (220) peaks decreases with increase of boron concentration from 0.2 M to 0.4 M. This behaviour can be understood by two computing processes; the increase of boron doping improves the stoichiometry of the films and increase of the crystal quality. This indicates that boron ions are substituted at manganese ions sites up to 0.1 M boric acid concentration after that B–B intragrain cluster is evaluated.

XRD pattern of highly doped (0.2 M and 0.4 M) MnO:B is shown in Fig. 1 and the inset shows the B–B cluster intragrain. It is observed that the XRD intensity depends strongly on the boron concentrations. The maximum of the XRD intensity is illustrated by the pronounced peak at a boric acid concentration of 0.1 M. Thus, increasing the dopant level results in a change in preferred growth in (111) and (220) direction.

The spray deposition of boric acid concentration of 0.1 M boron-doped MnO deposited at a substrate temperature of 375 °C is found to be optimal for the deposition of good quality B–MnO films at the specified spray

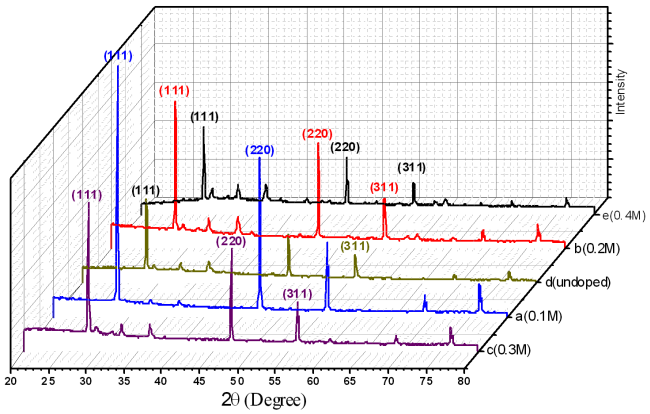

Fig. 1. XRD patterns of undoped and boron doped MnO films with the different concentrations of boric acid in the starting solution; (a) 0.1 M, (b) 0.2 M, (c) 0.3 M, (d) undoped, (e) 0.4 M.

conditions. It is shown that there is a critical doping value in the starting solution for which the characteristics of the MnO:B films has a minimal value, corresponding to the maximal crystal grain size value measured for these films. Consequently, the characteristics of B–MnO films prepared by the spray pyrolysis process depend strongly on the boron incorporation at the films, as similar behavior has been observed by Pawar et al. [21].

It is also shown in Fig. 1 that the initial increase in the XRD peaks can be explained by the creation of new nucleating centers due to the B dopant atoms. The subsequent decrease in the XRD peaks for the high doping level could be explained by two factors: firstly, by the saturation of the newer nucleating centers and secondly, due to the change in the energy absorption at the time of collision, and of the physical and chemical interaction between adatoms and the film. For boron doped films, the grain size initially increases with an increase in dopant contents (up to 1.0 M). Then, it is observed that the addition of boric acid contents increases the full width at half maximum (FWHM) due to the destruction of the crystal structure and reduction in the grain size. It may be possible that this drastic change in grain size is due to the large difference in ionic radius of manganese and boron. Thus, there is a decrease in the crystal grain size with the increase in the boric acid concentrations, which may be due to the sufficient increase in the supply of thermal energy for re-crystallization. Smaller crystallite size results in a higher density of grain boundaries, which behaves as barriers for carrier transport and traps for free carrier. Hence, a decrease of crystallite size can cause an increase of grain boundary scattering. This trend suggests that boron dopant creates newer nucleation centers, which in turn, would change the nucleation type from homogeneous to heterogeneous, and deteriorate the crystalline structure at high doping level.

The lattice constant a for the cubic phase structure is determined by the relation

$$a^2 = \frac{\lambda^2(h^2+k^2+l^2)}{4\sin^2\theta}, \quad (1)$$

where θ is the diffraction spectra Bragg angle, λ is the wavelength of the X-ray [22]. Lattice parameters for the undoped and boron doped MnO films are calculated using the relevant formula and systematically represented in Table I. The variation of the lattice constant with molar ratio of the boron doping on the MnO films are shown in Table I. The lattice constant a first decreases, reaches a minimum value around undoped MnO film and then appears to slowly increase with increase of the boron doped around the 5.3 and 5.4 Å as shown in Table I. The slow change in lattice constant for the spray deposited boron doped MnO film over the bulk clearly suggests that the film grains are strained which may be due to the nature and concentration of the native imperfections changing. The variation of the molar ratio of the boron in the MnO is associated with the changes in grain size and boundary.

TABLE I

XRD pattern results of the undoped and boron doped MnO films.

MnO doping	2θ [°]	Miller index	a [Å]	grain size [Å]	ε ($\times 10^{-3}$)	ρ [10^9/cm^3]
	28.4098	(111)	5.385	1.2039	3.2178	6.686
	47.2858	(220)	5.4327	1.2712	3.0642	6.379
undoped	56.0638	(311)	5.4362	1.2374	3.2869	6.123
	28.41	(111)	5.4371	1.2895	3.199	6.483
	47.3	(220)	5.4321	1.2969	3.029	6.324
0.1 M B	56.13	(311)	5.4303	1.2717	3.150	6.089
	28.4	(111)	5.4371	1.1842	3.2524	6.686
0.2 M B	48.1	(220)	5.346	1.2487	3.084	6.395
	56.06	(311)	5.4362	1.1188	3.442	6.1889
	28.52	(111)	5.4179	1.1606	3.2759	6.7083
0.3 M B	48.02	(220)	5.3545	1.2400	3.1508	6.3974
	56.74	(311)	5.3790	1.0742	3.4855	6.2342
	28.36	(111)	5.4468	1.0810	3.441	6.775
0.4 M B	47.2858	(220)	5.4327	1.1843	3.252	6.4232
	56.06	(311)	5.4361	1.0617	3.6645	6.2889

It is observed that the XRD patterns of the undoped and boron doped MnO films show a most preferred orientation along (111), (220) and (311) planes. The grain size of all films were estimated for the planes by using the Scherrer formula [23]:

$$d = \lambda/(D\cos\theta), \quad (2)$$

where d is the grain size, λ is the X-ray wavelength used, D is the angular line width of the half maximum intensity and θ is the Bragg angle. Table I shows the various grain parameters of the undoped and boron doped MnO films which are associated to the (111), (220) and (311) peaks. From these results, the boron concentration increases to 0.1 M concentration, the intensity of MnO peaks increases, and this peak becomes narrower indicating an improvement of the crystallinity. This means that the grain size of the films increases with increasing up to 0.1 M concentration of the boric acid. Then the boron concentration increases from 0.2 M to 0.4 M concentration of the boric acid, the intensity of MnO peaks decreases, and this peak becomes larger due to the destruction of the crystal structure and reduction of the grain size. The XRD intensity depends strongly on the permitted boron concentration. Maximal XRD intensity is illustrated by the pronounced peak with dopant contents (0.1 M concentration of boric acid). It is shown that the decrease in the grain size is correlated with the broadening of the XRD peak.

Smaller crystallite size results in a higher density of grain boundaries, which behaves as barriers for carrier transport and traps for free carriers. Hence, a decrease in the crystallite size can cause an increase in the grain boundary scattering [24]. This observation correlates with the results of XRD patterns. Consequently, the characteristics of the undoped and boron doped MnO films prepared by the spray pyrolysis process depend strongly on the boron incorporation at the films. It is also shown that the initial increase in the XRD peaks can be explained by the creation of new nucleating centers due to the B dopant atoms. In addition, it is observed also that the grain size initially increases with an increase in dopant contents (up to 0.1 M). Thus, it is observed that the grain size initially increases with an increase in dopant contents (up to 0.1 M). Then, the grain size of these films decreases for higher doping level. It is concluded that the crystallinity of the films increases with increase in grain size, which indicates a lower number of lattice imperfections. This may be due to a decrease in the occurrence of grain boundaries because of an increase on the grain size of the film with increase of boron concentration up to 0.1 M concentration of boric acid. These parameters indicate the formation of high quality B–MnO films deposited on the well cleaned glass substrate by spraying pyrolysis method with dopant contents (up to 0.1 M).

Misfit stresses occur in crystalline films due to the geometric mismatch at interphase boundaries between crystalline lattices of films and substrate. Therefore, a stress is also developed in the film due to the lattice misfit [25]. However, the stress has two components: thermal stress arising from the difference of expansion coefficient of the film and substrate and internal stress due to the accumulating effect of the crystallographic flaws that are built into the film during deposition. The average stresses of the deposited films are found to be compressional in nature. The compressive stress is due to the grain boundary effect, which is predominant in polycrystalline film [26]. Compressive stress is also likely to be due to the native defects arising from the lattice misfit. Native imperfections probably migrate parallel to the film substrate with their surface mobility modified by the substrate temperatures. The origin of the strain is also related to the lattice misfit which in turn depends upon the deposition conditions.

The microstrain (ε) developed in the sprayed MnO:B films were calculated from equation [27]:

$$\varepsilon = \frac{D\cos\theta}{4}, \tag{3}$$

where D is the full width at half maximum of the (100), (002) and (101) peaks and given in Table I. Table I shows the variation of the microstrain (ε) with boron concentration in MnO:B films. It is observed from Table I that the microstrain (ε) decreases with increase of the boric acid concentration up to 0.1 M. This type of change in microstrain may be due to the predominant recrystallization process in the polycrystalline films and due to the movement of interstitial Mn atoms from inside the crystallites to its grain boundary which dissipate and lead to a reduction in the concentration of lattice imperfections [28].

Also it is observed that the microstrain decreases with increase of the grain size of the films. This can be attributed to the improvement in crystallinity due to the regular arrangements of atoms in the crystal lattice and which can be correlated with the XRD results.

Moreover one can also notice that the microstrain decreases with the increase of boric acid concentration up to 0.1 M and then increases with the increase of boric acid concentration. It is clear from Table I that there occurs a decrease in internal microstrain within the film and an increase in the crystallite size.

Dislocations are an imperfection in a crystal associated with the misregistry of the lattice in one part of the crystal with respect to another part. Unlike vacancies and interstitial atoms, dislocations are not equilibrium imperfections, i.e. thermodynamic considerations are insufficient to account for their existence in the observed densities. In fact, the growth mechanism involving dislocation is a matter of importance. In this study, the dislocation density is determined from Williamson's and Smallman's method using the following relation for cubic MnO and boron doped MnO films [27] and the variation of the dislocation density with boron concentration is shown in Table I:

$$\rho = \frac{15\varepsilon}{aD}. \tag{4}$$

The dislocation density (ρ) is defined as the length of dislocation lines per unit of the crystal, and small ρ means that the crystallization of the films is good. As seen from Table I, ρ decreases with the increase of boron concentration up to 0.1 M and then increases with the increase of boron concentration. It is clear from Table I that there occurs a decrease of a number of lattice imperfections within the film and an increase in the crystallite size. This may be due to a decrease in the occurrence of grain boundaries because of an increase in the grain size of the film with increase in boric acid concentration up to 0.1 M. These parameters indicate the formation of high quality boron doped MnO films deposited on the well cleaned glass substrate by the spray pyrolysis method with dopant contents (up to 0.1 M). This can be attributed to the improvement in crystallinity due to the regular arrangements of atoms in the crystal lattice. Therefore, it could be also related to an improvement of the crystallinity leading to a decrease of donor sites trapped at the dislocations and grain boundaries. Also it is observed that the grain size decreases due to the increase of the dislocation density and the microstrain at the higher doping level. Since the dislocation density and the microstrain are the manifestation of dislocation network in the films, the increase in the microstrain and the dislocation density indicates the formation of lower quality films at upper boron doping level [29]. From the above results, it is concluded that boron doping plays an important role in the crystal orientations of MnO films and effectively modifies the microstructure of the MnO films.

3.2. Optical studies

Undoped and boron doped MnO films are direct transition semiconductors and their absorption coefficient (α) and optical band gap energy (E_g) are interrelated [30]. The band gap energy of the films was calculated from the $(\alpha h\nu)^2$ versus $h\nu$ (photon energy) which is plotted in Fig. 2. The plots are parabolic in nature and the number of inflexions reveals the number of transitions. The absorption coefficient as a function of photon energy was calculated and plotted for allowed direct transitions (neglecting exciton effects) by using the expression [30]:

$$\alpha h\nu = A(h\nu - E_g)^{1/2}, \tag{5}$$

where $h\nu$ is the photon energy, E_g denotes the optical energy bandgap, and A — the characteristic parameter (independent of photon energy) for respective transitions.

Figure 2 shows that the dependences of $(\alpha h\nu)^2$ as a function of photon energy $h\nu$ indicate the direct nature of band-to-band transitions for the studied samples with the boric acid concentration in solution with (a) 0.1 M, (b) 0.2 M, (c) 0.3 M, (d) undoped, and (e) 0.4 M.

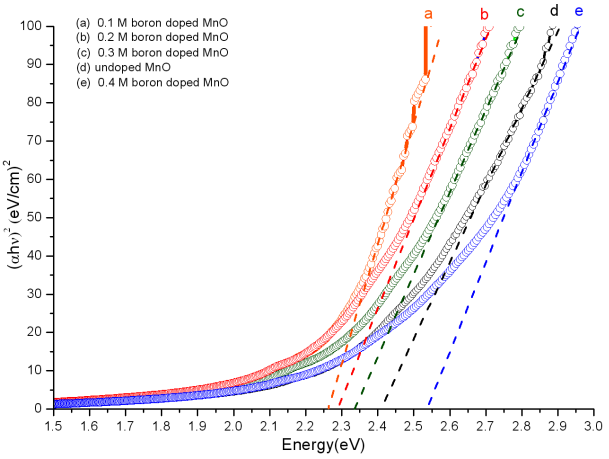

Fig. 2. A representative graph showing the dependence of $(\alpha h\nu)^2$ on the photon energy $h\nu$.

Table II gives the optical band gap values obtained by extrapolating the linear portion of the plots of $(\alpha h\nu)^2$ versus $(h\nu)$ to $\alpha = 0$. It is observed that the decreases

TABLE II

Band gap energies of the undoped and boron doped MnO films at 375 °C.

Molarity of B concentration [M]	Energy gap [eV]
0	2.41
0.1	2.25
0.2	2.28
0.3	2.34
0.4	2.54

in the optical band gap of the films with an increase in dopant contents (up to 0.1 M) can be attributed to the increase in the grain size. Another reason could be the improving crystallinity with increasing grain size and this may be due to the extension of electronic states of the impurity phase, precipitates and clusters, into the band gap of MnO:B. It is seen at higher doping levels that the band gap was increased, and the grain size of MnO:B films was decreased.

A similar behavior was observed in ZnO:Cu films deposited by spray pyrolysis method [22]. The change in E_g with the boron concentrations in solution and grain size was observed in MnO:B films. Therefore, the band gap energy shift of MnO:B films in our study can be attributed to the quantum size effect. The change in E_g with boron concentrations in solution can be understood by the quantum size effect observed in the films of semiconductors. Therefore, the optical band gap (E_{opt}) of doped MnO is broader than that of undoped manganese oxide films. It may be also another reason that defects are accumulated at the grain boundaries. Smaller grain size results in a tensile strain arising from thermal mismatch between the MnO film and the substrate. This indicates that the presence of large number of grain boundaries increases the defects in the film. Therefore, the change in E_g with boric acid contents can be correlated with the change of the structural properties of the films.

4. Conclusions

The study of the structural and optical properties of undoped and doped MnO films obtained by the spray pyrolysis technique shows that they are strongly dependent on the boron concentration. Particularly, it is observed that the best crystallinity of MnO films is obtained at the boron concentration of 0.1 M in solution. The films have polycrystalline structures and show a preferential orientation along (111), (220) and (311) planes with well-defined microstructures. B incorporation (at 0.1 M) caused the crystallinity levels to increase. The crystallization level is low at higher doping level between 0.2 M and 0.4 M due to the increasing grain boundaries which behave as defects in the structure affecting the structural properties of the films. From the XRD analyses it was concluded that B incorporation plays a significant role in the crystalline and structural properties of the MnO films and the formation of high quality B–MnO films deposited on the well cleaned glass substrate by spraying pyrolysis method with dopant contents (up to 0.1 M).

References

[1] J. Poortmans, V. Arkhipov, *Thin Film Solar Cells Fabrication, Characterization and Applications*, Wiley, Chichester 2006.

[2] M. Ortega-Lopez, A. Morales-Acevedo, *Thin Solid Films* **330**, 96 (1998).

[3] J.M. Peza-Tapia, V.M. Sanchez-Resendiz, M. Alb or-Aguilera, J.J. Cayente-Romero, L.R. De Leon-Gutierrez, M. Ortega-Lopez, *Thin Solid Films* **490**, 142 (2005).

[4] N. Badera, B. Godbole, S.B. Srivastava, P.N. Vishwakarma, L.S. Sharath Chandra, J. Deepti, V.G. Sathe, V. Ganesan, *Sol. En. Mater. Sol. Cells* **92**, 1646 (2008).

[5] S.A. Mayen-Hernandez, S.J. Sandoval, R.C. Perez, G.T. Delgado, B.S. Chao, O.J. Sandoval, *J. Cryst. Growth* **256**, 12 (2003).

[6] J. Mu, Z.F. Gu, L. Wang, Z.Q. Zhang, H. Sun, S.Z. Kang, *J. Nanopartic. Res.* **10**, 197 (2008).

[7] Z. Pingtang, Z. Qiumei, H. Xianliang, T. Hao, H. Kaixun, *J. Cryst. Growth* **310**, 4268 (2008).

[8] L. David, C. Bradford, X. Tang, T.C.M. Graham, K.A. Prior, B.C. Cavenett, *J. Cryst. Growth* **251**, 591 (2003).

[9] E. Jahne, O. Goede, V. Weinhold, *Phys. Status Solidi B* **146**, K157 (1988).

[10] H.M. Pathan, S.S. Kale, C.D. Lokhande, S.H. Han, O.S. Joo, *Mater. Res. Bull.* **42**, 1565 (2007).

[11] D.B. Fan, H. Wang, Y.C. Zhang, J. Cheng, B. Wang, H. Yan, *Mater. Chem. Phys.* **80**, 44 (2003).

[12] D. Fan, X. Yang, H. Wang, Y. Zhang, H. Yan, , *Physica B Condens. Matter* **337**, 165 (2003).

[13] S. Sur, Z. Öztürk, M. Öztas, M. Bedir, Y. YÖzdemir, *Phys. Scr.* **84**, 015701 (2011).

[14] J.C. Nardi, *J. Electrochem. Soc.* **132**, 1787 (1985).

[15] L. Sanchez, J. Faray, J.P. Pereira-Ramos, L. Hernan, J. Morales, L. Tirado, *J. Mater. Chem.* **6**, 37 (1996).

[16] R.N. Reddy, R.G. Reddy, *J. Power Sourc.* **132**, 315 (2004).

[17] R.N. Reddy, R.G. Reddy, *J. Power Sourc.* **156**, 700 (2006).

[18] C.N. Xu, K. Miyazaki, T. Watanable, *Sens. Actuat. B* **46**, 87 (1998).

[19] K.J. Kim, Y.R. Park, *J. Cryst. Growth* **270**, 162 (2004).

[20] B.D. Cullity, S.R. Stock, *Elements of X-ray Diffraction*, 3rd ed., Prentice Hall, New Jersey 2001.

[21] B.N. Pawar, S.R. Jadkar, M.G. Takwal, *J. Phys. Chem. Solids* **66**, 1779 (2005).

[22] M. Öztas, M. Bedir, *Thin Solid Films* **516**, 1703 (2008).

[23] K.J. Kim, Y.R. Park, *J. Cryst. Growth* **270**, 162 (2004).

[24] M. Bedir, M. Öztaş, S.S. Çelik, T.T. Özdemir, *Acta Phys. Pol. A* **126**, 840 (2014).

[25] I.A. Ovid'ko, *Rev. Adv. Mater. Sci.* **1**, 61 (2000).

[26] I.M. Khan, in: *Handbook of Thin Film Technology*, Eds. L.I. Maissel, R. Gland, McGraw-Hill, New York 1970, Ch. 10.

[27] M. Bedir, M. Oztas, O.F. Bakkaloglu, R. Ormancı, *Eur. Phys. J. B* **45**, 465 (2005).

[28] F.A. Kroger, *The Chemistry of Imperfect Crystals*, North-Holland, Amsterdam 1964.

[29] N. Jabena Begum, K. Ravichandrann, *J. Phys. Chem. Solids* **74**, 841(2013).

[30] O.S. Heavens, *Optical Properties of Thin Solid Films*, Dover, New York 1965.